Non-destructive characterization of archaeological resins: seeking alteration criteria through vibrational signatures

Céline Daher, Ludovic Bellot-Gurlet

1 **Non-destructive characterization of archaeological resins: seeking alteration criteria**

2 **through vibrational signatures**

3

4 Céline Daher [1], Ludovic Bellot-Gurlet [1,*]

5

6 [1] Laboratoire de Dynamique, Interactions et Réactivité (LADIR), UMR 7075 CNRS - UPMC

7 Université Pierre et Marie Curie Paris 6, 4 place Jussieu 75005 Paris, France. E-mail:

8 cel.daher@gmail.com, ludovic.bellot-gurlet@upmc.fr; Tel : +33 1 44 27 36 18 ; Fax : +33 1

9 44 27 30 21

10

11

12 **Abstract**

13   Natural resins are prone, as all natural organic products, to ageing and degradation.

14 Characterizing this alteration provides a better knowledge about their chemistry, and when

15 they are involved in cultural heritage artefacts, it helps to define relevant conservation

16 protocols. In this study, a set of archaeological African copals that present specific surface

17 degradations and colors were analyzed by FT-Raman and ATR-IR spectroscopies. A

18 methodology based on the modifications of the vibrational features between the bulk and the

19 resins surface was define. A relation between the evolution of the molecular structure of the

20 copal samples and some vibrational bands could be established; and possible ageing reactions

21 occurring at the surface of the samples could be proposed. This specific surface aspect is

22 actually related to an alteration, and the surface states and the colors variability are linked to

23 different alteration degrees. This could refer to whether different conservation contexts

24 (presence of air, water, etc), possible preparation or different origins: for example the

25 collection of fresh or partly fossilized resins.

26

27 **Keywords**

28 FT-Raman, ATR-Infrared, archaeological resins, copal, ageing, spectral decomposition

29

30

31 **A. Introduction**

32   Natural resinous substances have been used, across time, for different purposes, and in

33 different forms: in their raw form, such as frankincense or myrrh as incense [1], or amber and

34 copal for jewellery [2,3]; or different tree exudates for healing purposes or religious ceremonials

35   [4,5]. They also have been used after some treatments (heating, mixtures): as adhesives [6,7] or

36   waterproofing materials for ceramics [8] or ship building [1,9] and finally as binders for paint [10] or

37   part of a varnish composition [11,12].

38   Besides, as all natural substances, resinous materials are highly exposed to ageing and

39   degradation, which constitute an issue when it comes to Cultural Heritage artefacts. It is thus

40   important to characterize the alteration and degradation processes in order to have, on one

41   hand, a better understanding of the past and present chemistry of these substances; and to be

42   able, on the other hand, to make viable and accurate diagnoses about their conservation state.

43

44   The identification of such substances is usually done by separative techniques often

45   coupled to mass spectrometry [13,14] which nevertheless require a destructive sampling and a

46   reasoned choice of analytical and/or pre-treatment conditions. However, working on cultural

47   heritage artefacts often requests non destructive techniques that perform rapid analyses with

48   slight experimental constraints. Vibrational spectroscopies are increasingly employed for

49   identification purposes by setting up reference databases, [15,16] or to give spectroscopic clues to

50   differentiate between organic substances [17,18,19,20,21,22] with some specific studies on

51   archaeological resins [23,24]. Indeed, when ancient organic materials are involved, the question

52   of ageing and degradation is raised. The molecular modifications cause changes in the

53   vibrational signatures, and it becomes difficult to define spectral databases of substances that

54   evolve over time [25].

55

56   Previous studies using Raman spectroscopy [4,26,27] tried to find ageing criteria for

57   natural resins mostly based on two bands intensity ratio (I_{1650}/I_{1450}) that evolves from a fresh

58   resin to an aged one. However they have based their work on a corpus of resins from different

59   chemical families, origins, size and aspects. This large variety of parameters complicates the

60   study; their respective influence is difficult to demonstrate.

61

62   This study focuses on artefacts with the same chemistry and origin, found in a same

63   excavation site from the 13th century: copals from Africa and/or Madagascar found in Sharma

64   (Yemen) [28]. Besides, the altered and unaltered analyzed materials are part of a same sample,

65   since their surface seems degraded, and the core of the resins has a fresh transparent aspect.

66   Furthermore, among all the copals found in this excavation site, three groups could be

67   formed, based on their colors and aspects. This difference in the appearance might be related

68   to different surface alteration states, and was the motivation for this work. We tried then to get

69 chemical information about the alteration processes with samples matching different stages of

70 the copal ageing.

71

72   In this work, FT-Raman and IR-microATR analyses were performed on a set of

73 copals, whether on the internal or external samplings. We applied the I_{1650}/I_{1450} ratio as an

74 ageing criterion but the obtained trend was opposite to the one obtained by Winkler *et al.*[26]. In

75 order to understand this evolution and to get more precise degradation criteria, but also to

76 propose some chemical interpretations to the spectral changes, spectral decomposition

77 calculations were performed on different regions of the Raman and IR spectra. Finally, some

78 hypotheses on the chemical evolution of the copals molecular structures are presented, and a

79 progression of the ageing with the colors and surface aspects of the resins is highlighted with

80 a proposition of new indexes.

81

82

83 **B. Analyzed material**

84 **B.1. Samples**

85   Ten samples of archeological copal from a medieval site in Sharma (Yemen) [28,29] have

86 been analyzed. They have been previously identified as eastern African and/or Madagascar

87 copals by their molecular markers thanks to GC/MS and py-GC/MS [30]. This ensures, for the

88 archaeological studied samples, a same biological origin and hence identical chemical

89 characteristics. It is thus possible to attempt reliable statements about their degradation

90 processes. These artefacts are raw fragments of copal which have a same hard and transparent

91 bulk but different surface states and colors (Fig. 1): from yellow fragments with a thin dry

92 surface, to orange fragments with a flaked-off surface and finally red fragments with a thick

93 and very friable surface. Moreover, all the samples are wholly preserved, even sometimes

94 with traces of sediments.

95

96   For these archaeological copals, a specific analyzing procedure was applied: small

97 flakes from the internal and external parts of each artefact were sampled and separately

98 analyzed to take into account this heterogeneity. Since the implemented analyses are non-

99 destructive, each flake could be analyzed by FT-Raman then IR-microATR. For each

100 fragments several points were analyzed and the very similar spectra were averaged in order to

101 improve the signal-to-noise ratio.

102

B.2. Chemical composition

103

104 African and Madagascar copals are diterpenic resins that exude from trees of the

105 *Leguminosae* family, and have as major components copalic and cis-ozic acids (Fig. 2) based

106 on a labdane type skeleton [31]. Copals are known to be highly polymerized resins, and most of

107 the time, a pyrolysis step is needed for the separative methods analyses [32,33].

108

109

C. Instrumentation

110

C.1. Raman spectroscopy

111

112 To overcome the high fluorescence of such organic samples which prevent the

113 observation of Raman scattering, we favor a near infrared excitation at 1064 nm from an Nd-

114 YAG laser diode. The FT-Raman spectrometer is a Bruker RFS 100/S based on a Michelson-

115 type interferometer and equipped with a liquid nitrogen-cooled Ge detector.

116

117 The samples were analyzed using a microscope interface with a 40x IR objective,

118 allowing a spot size of 30 µm approximately. In order to improve the collected Raman signal

119 intensity, the samples were placed on a gold mirror. Laser power at the sample was adjusted

120 at 250 mW (nominal power of 500 mW) and no damage or heating of the materials was

121 observed. Spectra were recorded between 3500 and 50 cm^{-1} with a 4 cm^{-1} resolution and a low

122 signal-to-noise ratio was achieved by accumulating 1500 scans.

123

C.2. Infrared spectroscopy

124

125 Non destructive micro-infrared spectroscopy analysis is carried out in micro

126 Attenuated Total Reflectance mode (IR-microATR). Measurements by contact were

127 performed with a 100 µm diameter Germanium crystal tip (mono-reflection) fixed on the 20x

128 objective of an IRscope II microscope which also allows the visualization of the analyzed

129 area. The microscope is linked to a Bruker Equinox 55 spectrometer equipped with a liquid

130 nitrogen-cooled MCT detector. Spectra between 4000 and 600 cm^{-1} with a 4 cm^{-1} resolution

131 were recorded with 200 scans accumulated.

132

133

D. Ageing characterization: methodology, results and discussion

134

135

D.1. The "vibrational features/molecular structures" relation

136

Spectra from internal and external fragments were first compared to underline their main differences and the effect of degradation on their molecular structure. Figure 3 presents the FT-Raman and IR-ATR spectra representative of an externally red archaeological copal. On the FT-Raman spectrum (Fig. 3 a)) of the external part of the copal grain, in addition to a light fluorescence background due to the intense color of the surface, the bands are less intense and broader than the internal part one. The most important differences are located in the $1650\text{-}1500$ cm^{-1} region assigned to the stretching vibrations of the CC double bonds. Another region shows some decrease in the intensity, the CH stretching vibration massif, around 2900 cm^{-1}. For the IR spectra (Fig 3 b)), some bands decrease, for example the band at 887 cm^{-1} assigned to the bending vibration of the CH bonds in vinyl groups, others increase, especially a band around 1580 cm^{-1}, assigned to the C=C stretching vibration of aromatic groups. The alteration has also an impact on the CH stretching massif of the IR spectra, specifically the band at 3075 cm^{-1} assigned to CH bonds in vinyl groups.

The various observations made on the FT-Raman and IR spectra global profiles of a red copal underline the chemical transformations that occurred within the copal surface. These modifications can be considered as alteration, and can also be related to the color of the resin: more colored is the sample, more altered it will be. Moreover, it is correlated to the sample surface aspect, from dry in appearance to brittle, highlighting a mechanical de-cohesion derived from a chemical transformation. It is thus interesting to have an improved description and a better understanding of these spectral evolutions, and try to find specific alteration criteria that can be easily obtained.

D.2. Seeking degradation criteria

Previous studies showed the possibility of characterizing the maturation of such resins using Raman spectroscopy, by a band intensity ratio: the stretching vibration of the C=C bonds band around 1650 cm^{-1} with the deformation vibration of the C-H bonds band around 1450 cm^{-1} [26,27]. We have already seen that the latter does not show an important intensity variation with degradation, but the former is highly influenced by the alteration process and significantly decreases. However this ratio has different meanings according to the different cited studies. Winkler *et al.*[26] underline that the resin is rather "fresh" or unaltered for higher intensity ratio ($I_{\nu C=C}/I_{\delta C-H}$) values, and that this ratio decreases with the sample age. Brody *et al.*[27] present the same ratio variation, but do not properly link it with the samples age. They

170   evoke the influence of environmental factors in the resins evolution, as well as the influence

171   of the different chemical compositions from a diterpenic resin to another (botanical origin).

172

173   The comparison between the internal and external parts of the studied copals shows an

174   inverse trend in this ratio (see Table 1 and Fig. 4). First, for the internal parts of the ten

175   samples, the ratio is located between 0.89 and 1.15 with a mean value at 1.05 for a standard

176   deviation of about 9%. According to Winkler *et al.*[26], all our copals have about the same age.

177   According to Brody *et al.*[27], this very similar index value underlines comparable chemical

178   states, which is consistent with the attested origin of our eastern Africa and/or Madagascar

179   copals. However, both papers [26,27] do not specify the analyzed part of the samples (surface,

180   bulk, or possible heterogeneities), but since they are interested by representative samples, we

181   assume that only the "bulk" of their samples was considered. In our study, only one kind of

182   resinous material was selected: same chemistry [30] and thus same geological origin.

183   Furthermore, our aim is to compare the internal and external altered parts in order to follow

184   this degradation process. The expected results are therefore not related to the age, the

185   maturation or fossilization processes of the resin.

186

187   By comparing the index values for the external parts of the three groups of copals, it

188   can be noticed first that for the yellow samples, the ratios for the external samplings are

189   consistently lower than for internal ones. However, the ratio for the external samplings

190   increases significantly from yellow to red samples (from 1 to 1.76), according to the

191   established degradation progression. A deeper look at the Raman bands profile of the copals

192   external parts (Fig. 4) in the 1800-1400 cm^{-1} region, highlights a stable shape the 1500-1400

193   cm^{-1} area, while significant differences can be observed in the 1700-1500 cm^{-1} region. For the

194   yellow copals, the C=C stretching band is less intense (Fig. 4 a) and b)), and seems slightly

195   larger than the internal part spectra. For the orange copals (Fig. 4 c)), the 1650 cm^{-1} massif

196   increases; and finally get very intense and broad for the red copals (Fig. 4 d)) with a

197   maximum shifted to 1580 cm^{-1}. We can thus underline a clear global increase of the intensity

198   of the I_{1650}/I_{1450} ratio related to the surface degradation state of these copals. This ratio index

199   is here considered as an alteration marker of the samples surface. Besides, the evolution of the

200   index all along the degradation process is not strictly linear, since a slight decrease is

201   observed between the external and internal parts of the less altered samples (yellow copal).

202

203   However, even if this index is easily calculated and appears to be related with the

204   degradation state, more detailed information about the chemical processes that occur should

205   be extracted thanks to a deeper analysis of the bands profile.

206

207   **D.3. Spectral decomposition, finding a general pattern**

208

209   *D.3.1. Fingerprint spectral region*

210   A specific methodology for the spectral decomposition process was adopted, with the

211   aim of monitoring the bands evolution, and trying to define the bands, and thus the specific

212   bonds, that are most affected by the ageing. It was first applied on the fingerprint region

213   (1800-1400 cm^{-1}) since it seems to undergo several modifications, especially on the FT-

214   Raman spectra. The spectra of all the internal and surface samples were truncated between

215   1925 and 1395 cm^{-1}, then a linear baseline was subtracted (set points: 1925, around 1515 and

216   1395 cm^{-1}) and finally the cut spectra were normalized on the 1450 cm^{-1} massif intensity,

217   since it appears unchanged with the resin ageing (Opus software, Bruker).

218

219   The decomposition procedure (Asrel2 homemade software, LADIR) was defined

220   according to several parameters: the number of bands and their position (P), the area (A), the

221   full width at half maximum (W) and the profile (K) of the band (which equals 0 if Gaussian, 1

222   if Lorentzian). The number and initial positions of the bands were determined by calculating

223   the second derivative of the massif for each spectrum. Each minimum on the derivative

224   indicates the position of a band. The same number of bands (11 bands) was defined for the

225   internal and surface samples, 7 bands in the C=C vibration massif, and 4 bands in the C-H

226   deformation massif. Concerning the adjustment procedure, it is based on a least squares

227   method which adjusts the band parameters to fit the experimental spectrum.

228

229   Figure 5 illustrates the results of this procedure. For all the 10 internal samples, the

230   decomposition result was the same, thus only one is presented (Fig. 5 a)). In general, for

231   external samples same number of bands was obtained for all the fittings, but their position and

232   profile differ from a sample group to another. Figure 6 shows a graph representing the

233   evolution of the bands position between the surface sample fitting results and the internal

234   sample ones, for the 3 groups of copals. For external samples (Fig. 5 b) to d)), it can be easily

235   noticed that the positions of the 4 bands related to the C-H deformation massif are not really

236   changing (bands 1 to 4), in contrast to the bands 5 to 11 that undergo important shifts

237 especially for the orange and red copals. Using this spectral region for the study of the resins
238 ageing is therefore currently compromised by the difficulty of finding an objective generic
239 fitting pattern for the Raman spectra of the internal and external parts. It is thus difficult to
240 distinctly underline and follow the bands that evolve with the resin alteration, and even harder
241 to link this evolution to specific vibrators in this spectral region.
242
243 *D.3.2. CH massif region*

244   It was therefore necessary to focus on another spectral area that show an evolution of
245 its vibrational features with the resin alteration, in order to point out these bands and then
246 correlate these changes to chemical modifications at the resins surface. As it was said before,
247 the CH stretching vibration massif (centered at 2900 cm^{-1}) present several variations, whether
248 on the IR or FT-Raman spectra. This region has been less studied, but can be very informative
249 for substance discrimination [34, 35], or to assess if its features evolutions are characteristics of
250 some organic binders alteration [36].
251
252   The previous spectral decomposition methodology was applied to this region: the
253 spectra have been truncated, baseline subtracted, normalized, and finally fitted with 7 bands
254 as observed on the second derivative for both Raman and IR spectra and all samples (see
255 example on Fig. 7). It can be noticed that the minima observed on the second derivatives are
256 in the same positions for the internal and external fragments spectra. These 7 bands
257 (numbered from 12 to 18 to avoid any confusion with the 1800-1400 cm^{-1} region bands) are
258 assigned to C-H bonds in different chemical groups or environments: band 12 is assigned to
259 $\nu(CH)_s$ in CH_2 groups; bands 13 and 14 to $\nu(CH)_s$ in CH_3 or CH groups; band 15 to $\nu(CH)_{as}$ in
260 CH_2 groups; band 16 to $\nu(CH)_{as}$ in CH_3 groups; band 17 to $\nu(CH)$ in aromatic groups; and
261 finally band 18 to $\nu(CH)$ in vinyl groups.
262
263   Comparing internal and external samplings signatures, the bands that generally vary
264 the most are bands 12 and 18, at respectively 2849 and 3081 cm^{-1} for Raman and IR data (Fig.
265 7 c), colored bands). These two bands decrease significantly: indeed the 2849 cm^{-1} band that
266 appears thin and relatively intense on the internal fragment spectrum, is more like a shoulder
267 on the external sample spectrum; and the 3081 cm^{-1} band seems to decrease and gets broad,
268 and tends to disappear. In order to quantify and characterize the spectral modifications, the
269 fitting parameters (A, W and K) of the internal and external samples have been taken into
270 account. Since the bands positions (P) are the same for the internal and external samples

271 spectra, it was not taken into account for these calculations. Figure 8 represents the calculated
272 differences for the areas (A) and the width at half maximum (W). Globally, the parameters do
273 not show the same progress for all the bands. For Raman and IR data, the A and W
274 parameters of bands 14 and 15 present an about 10% variation between the surface and the
275 core of the resins: these two bands are in the middle of the CH stretching massif, and are not
276 strongly affected by the resin ageing. Bands 12 and 18 are the most affected by the surface
277 alteration: the areas are highly decreasing (up to 80% for band 18 on the IR spectra), and the
278 widths at half maximum are increasing (up to 100% for band 18). These remarks are directly
279 related to previous qualitative observation on the spectra fittings: if a band decrease and gets
280 broader, its intensity necessarily decreases. Finally, A and W for bands 13 and 17 are slightly
281 increasing: it is probably due to the fitting procedure during which the bands fulfill the massif
282 ends to optimize the spectral adjustment. Finally, figure 8 shows that the extreme values for
283 the relative differences are for the red copals, which are the most altered resins of the corpus.
284 The last parameter, K the band profile, tends to decrease for all the bands and all the samples,
285 evolving towards a Gaussian profile.
286
287

288 **D.4. Ageing and degradation: chemical interpretation**
289   Band 18 is the most changing band and is assigned to CH vibrations in exocyclic CC
290 double bonds which are highly present in the copal major components molecular structure
291 (see Fig. 2). The important decrease of this band could be explained by an oxidation of the
292 C=C bonds, and a cyclization reaction. These phenomena can occur more or less moderate,
293 depending on the conservation environments: a resin exposed to the air is more prone to
294 oxidation then a buried resin in a dry and close climate. Such reactions can explain the
295 broadening of the 1630 cm^{-1} band on the Raman spectra and, on the IR spectra, the presence
296 of a band around 1580 cm^{-1}, and also the decrease of the 887 cm^{-1} band, assigned to the
297 bending vibration of olefinic CH. The two former observations can point out the formation of
298 conjugated C=C aromatic bonds, which also explain the shift of the 1650 cm^{-1} band to lower
299 wavenumbers; and the coloration of the samples surface as well.
300

301   Band 12 is assigned to the symmetric vibration of CH bonds in aliphatic CH_2 groups,
302 and shows a relatively significant variation which can be related to cyclization reactions
303 leading to the loss of CH_2 aliphatic chains; or, if the surface is highly altered, to chain
304 breaking, explaining the brittleness of the surface for some samples.

305

306   Finally, the decrease of the K parameter, describing the evolution to a Gaussian profile

307 of most of the bands, illustrates the emergence of disorder within the altered material. Indeed,

308 a vibrator has normally a Lorentzian shape, but when a kind of disorder appears (for example

309 random chain breakings) the vibrators are no longer identical because of the new different

310 structural environments. Their characteristics are then randomly dispersed around a mean

311 value, introducing a Gaussian feature in the band profile.

312

313   Alteration indexes can also be calculated or drawn based on the CH massif

314 decomposition parameters. Figure 9 shows two plots of different fitting parameters of the

315 external samplings spectra, involving the full width at half maximum of various bands. As

316 said before, bands 12 and 18 are the two bands that evolve the most within the CH massif, and

317 band 15 is the central and most intense one, and is the less influenced by the alteration.

318 Nevertheless, it evolves sufficiently to inform about the degradation state. We can notice, on

319 these two plots, that the samples are sorted along the diagonal according to their colors, with

320 an internal sample at the very beginning of the graphs, as a reference point. These parameters

321 (or ratios) can thus be considered as new degradation indexes involving the CH massif

322 features. It is thereby possible to monitor the copals alteration by considering the external

323 parts of the samples. With this new approach, it appears that sampling is not necessary to

324 characterize a sample degradation state; the analyses can be performed directly on the samples

325 surface in a totally non destructive way.

326

327

328 **E. Conclusion**

329   The study of a collection of ancient copal artefacts from the same family tree and

330 preserved in the same archaeological site allowed the observation of molecular scale

331 alterations thanks to non destructive FT-Raman and IR-microATR spectroscopies. These

332 artefacts, first classified by their apparent color (from yellow to red) and surface aspect (from

333 dry to pulverulent, respectively), were sampled at their surface and in their bulk, enabling a

334 direct comparison, and a characterization of their surface degradation. The restriction of the

335 study to this samples set has prevented the introduction of additional parameters (variability

336 of the chemical nature and uncertain origins) that can complicate the interpretations.

337

General observations of the vibrational signatures have underlined more important modifications of the molecular structure for the red copals than for the orange and yellow ones. The degradation state was first evaluated by FT-Raman using a previously proposed I_{1650}/I_{1450} ratio [26,27]. However, in our study, this ratio has a reverse evolution; lower values are obtained for less altered samples, and the index increases with the degradation state. This questions the chemical processes documented by this index. Is it related to long term fossilization processes affecting the whole sample, or some alterations starting from the surface? To meet some further detailed studies are required in order to specify the role of each parameter (chemistry, environment, time, etc) and their possible interactions.

Then, a relation between the copals molecular structures and the evolution of some vibrational features were investigated focusing of the spectral regions presenting the larger variations. Spectral decomposition was then implemented to identify and monitor the evolution of the bands assigned to specific structural features. A too important bands shift in the fingerprint region (1800-1400 cm^{-1}) has hampered the built up of a unique decomposition model according to the resins degradation; and therefore the precise identification of the concerned bands and chemical bonds. However, the treatment of the CH stretching region (3100-2800 cm^{-1}) has underlined bands variations that follow the resins degradation state. Hypotheses on the chemical evolution of copal with ageing were then proposed, as well as other indexes involving the CH massif.

Moreover, knowing that these copals found in Yemen are from eastern Africa and/or Madagascar, they are a testimony of the ancient commercial routes during the 13th century, and their aspects and their conservation states might then be related to specific collection and exploitation modalities. Are the resins freshly collected or gathered from partly fossilized deposits, or have they undergone some possible treatments? The conservation state could underline here if one or several geographical or technical origins are involved for these copals. Further studies with direct dating of the artefacts should bring further information.

Non destructive analytical approaches, with Raman and/or IR spectroscopies, could contribute to the study of resins degradation mechanisms, and propose ageing characterization and monitoring for conservation purposes. As resins are involved in various cultural heritage objects (in raw form, or in preparations as varnishes) such diagnostic tools could be easily implemented by respecting the conservation constraints.

References

1. Langenheim J.H., *Plant Resins: Chemistry, Evolution, Ecology, and Ethnobotany*, Timber Press, 2003.
2. de Faria D.L.A., Edwards H.G.M., Afonso M.C., Brody R.H. and Morais J.L., *Spectrochimica Acta Part A: Molecular and Biomolecular Spectroscopy*, 2004, **60**, 1505-1513.
3. Edwards H.G.M., *Analytical and Bioanalytical Chemistry*, 2010, **397**, 2677-2683.
4. Edwards H.G.M. and Falk M.J., *Spectrochimica Acta Part A: Molecular and Biomolecular Spectroscopy*, 1997, **53**, 2393-2401.
5. Edwards H.G.M., Villar S.E.J., David A.R. and de Faria D.L.A., *Anal. Chim. Acta*, 2004, **503**, 223-233.
6. Regert M., Alexandre V., Thomas N. and Lattuati-Derieux A., *J. Chromatogr. A*, 2006, **1101**, 245-253.
7. Shillito L.M., Almond M.J., Wicks K., Marshall L.J.R. and Matthews W., *Spectrochimica Acta Part A: Molecular and Biomolecular Spectroscopy*, 2009, **72**, 120-125.
8. Garnier N., Cren-Olive C., Rolando C. and Regert M., *Anal. Chem.*, 2002, **74**, 4868-4877.
9. Colombini M.P., Giachi G., Modugno F., Pallecchi P. and Ribechini E., *Archaeometry*, 2003, **45**, 659-674.
10. van den Berg K.J., Boon J.J., Pastorova I. and Spetter L.F.M., *Journal of Mass Spectrometry*, 2000, **35**, 512-533.
11. Doménech Carbó M.T., *Anal. Chim. Acta*, 2008, **621**, 109-139.
12. Le Hô A.-S., Duhamel C., Daher C., Bellot-Gurlet L., Paris C., Regert M., Sablier M., André G., Desroches J.-P. and Dumas P., *Analyst*, 2013, DOI 10.1039/C3AN00608E.
13. Evershed R.P., *Archaeometry*, 2008, **50**, 895-924.
14. Colombini M.P. and Modugno F., eds., *Organic Mass Spectrometry in Art and Archaeology*, Wiley-Blackwell, 2009.
15. Vandenabeele P., Wehling B., Moens L., Edwards H., De Reu M. and Van Hooydonk G., *Anal. Chim. Acta*, 2001, **407**, 261-274.
16. Edwards H.G.M., Farwell D.W. and D. L., *Spectrochimica Acta Part A: Molecular and Biomolecular Spectroscopy*, 1996, **52**, 1639-1648.

415   17.   Vandenabeele P., Ortega-Aviles M., Castilleros D.T. and Moens L., *Spectrochimica*
416   *Acta Part A: Molecular and Biomolecular Spectroscopy*, 2007, **68**, 1085-1088.

417   18.   Teodor E.S., Teodor E.D., Virgolici M., Manea M.M., Truica G. and Litescu S.C., *J.*
418   *Archaeol. Sci.*, 2010, **37**, 2386-2396.

419   19.   Brody R.H., Edwards H.G.M. and Pollard A.M., *Biopolymers*, 2002, **67**, 129-141.

420   20.   Derrick M., *Journal of American Institute for Conservation (JAIC)*, 1989, **28**, 43-56.

421   21.   Daher C., Paris C., Le Hô A.-S., Bellot-Gurlet L. and Echard J.-P., *J. Raman*
422   *Spectrosc.*, 2010, **41**, 1204–1209.

423   22.   Guiliano M., Asia L., Onoratini G. and Mille G., *Spectrochimica Acta Part A:*
424   *Molecular and Biomolecular Spectroscopy*, 2007, **67**, 1407-1411.

425   23.   Edwards H.G.M., Sibley M.G., Derham B. and Heron C.P., *J. Raman Spectrosc.*,
426   2004, **35**, 746-753.

427   24.   Shashoua Y., Berthelsen M.B.L.D. and Nielsen O.F., *J. Raman Spectrosc.*, 2006, **37**,
428   1221-1227.

429   25.   Edwards H.G.M. and Ali E.M.A., *Spectrochimica Acta Part A: Molecular and*
430   *Biomolecular Spectroscopy*, 2011, **80**, 49-54.

431   26.   Winkler W., Kirchner E.Ch., Asenbaum A. and Musso M., *J. Raman Spectrosc.*, 2001,
432   **32**, 59-63.

433   27.   Brody R.H., Edwards H.G.M. and Pollard A.M., *Spectrochimica Acta Part A:*
434   *Molecular and Biomolecular Spectroscopy*, 2001, **57**, 1325-1338.

435   28.   Rougeulle A., *Annales Islamologiques*, 2004, **38**, 201-253.

436   29.   Rougeulle A., Proceedings of the Seminar for Arabian Studies, 2005.

437   30.   Regert M., Devièse T., Le Hô A.-S. and Rougeulle A., *Archaeometry*, 2008, **50**, 668-
438   695.

439   31.   Mills J.S. and White R., *The Organic Chemistry of Museum Objects*, 2nd edn.,
440   Butterworth - Heinemann, 1994.

441   32.   Osete-Cortina L. and Doménech-Carbó M.T., *J. Chromatogr. A*, 2005, **1065**, 265-278.

442   33.   Chiavari G., Montalbani S. and Otero V., *Rapid Commun. Mass Spectrom.*, 2008, **22**,
443   3711-3718.

444   34.   Nevin A., Osticioli I., Anglos D., Burnstock A., Cather S. and Castellucci E., *Anal.*
445   *Chem.*, 2007, **79**, 6143-6151.

446   35.   Daher C., Bellot-Gurlet L., Le Hô A.-S., Paris C. and Regert M., *Talanta*, 2013, **115**,
447   540-547.

448   36.   Nevin A., Osticioli I., Demetrios Anglos D., Burnstock A., Cather S. and Castellucci
449   E., *J. Raman Spectrosc.*, 2008, **39**, 993-1000.

450
451
452

		$I\nu_{(C=C)} / I\delta_{(C-H)}$	
Sample		**Internal**	**External**
Yellow copals Dry surface	**MR1210**	0.94	0.83
	MR1212	0.89	0.85
	MR1211	1.09	0.94
	MR1213	1.13	1.07
Orange copals	**MS5673**	1.11	1.21
	MS5676	1.07	1.25
Red copals Pulverulent surface	**MR1225**	1.10	1.29
	MR1226	1.15	1.31
	MR1214	0.91	1.33
	MR1234	1.07	1.76

Table 1: Intensity ratio of the 1650 cm^{-1} / 1450 cm^{-1} massifs ($I\nu_{(C=C)}$ / $I\delta_{(C-H)}$) calculated for internal and external parts of 10 copals samples with different external aspects. The intensities were measured at the most intense point of each whole massif, and not at a specific wavenumber.

470

471

472
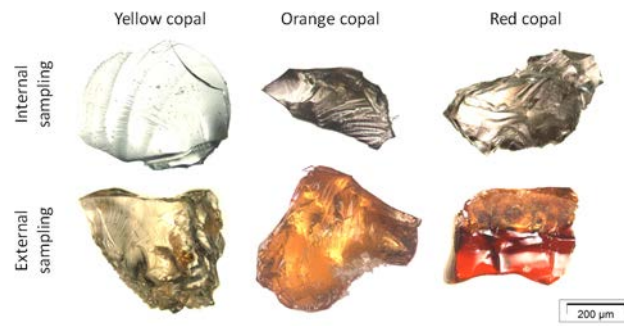
Fig. 1: Representative samples of the studied copals illustrating the external aspect variability
(Samples refs: MR1211, MS5673, MR1234).

475

476

Copalic acid   Ozic acid
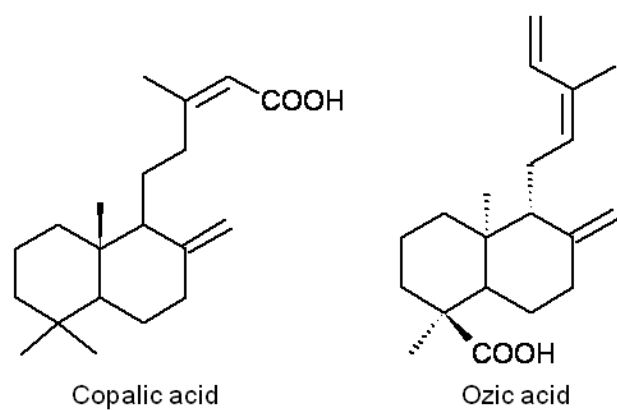
Fig. 2: Molecular structure of the majors components of Africa and Madagascar copals. See
text (part D.4) for a detailed description of the functions affected by alteration and monitored
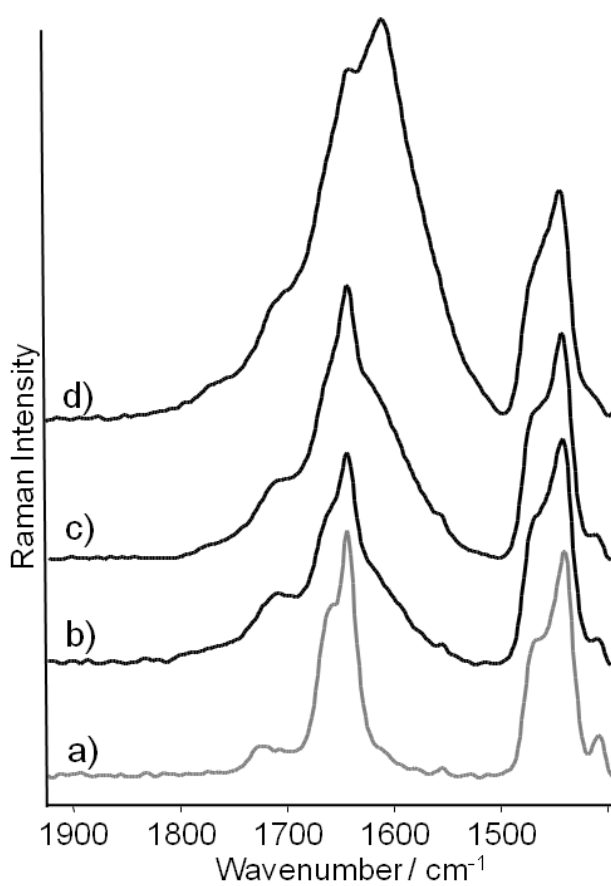by vibrational spectroscopy.

481

482

483
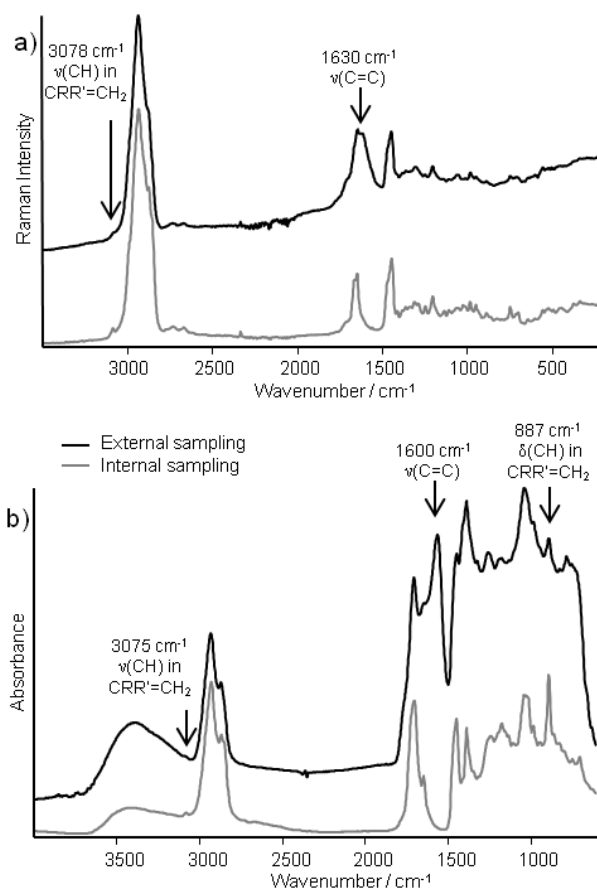
484

485 Fig. 3: a) FT-Raman and b) ATR-IR spectra from internal (gray line) and external (black line)

486 parts of an externaly red sample (Ref: MR1214).

487

488

489

490

491 Fig. 4: Representative FT-Raman spectra of 3 copals samples, one from each group: a) yellow

492 (MR1211) – internal sampling, b) yellow (MR1211) – external sampling, c) orange (MS5673)

493 – external sampling, and d) red (MR1234) – external sampling. The spectra have all been

494 normalized on the 1450 cm^{-1} band intensity in order to monitor the 1650 cm^{-1} band evolution.

495

496

497
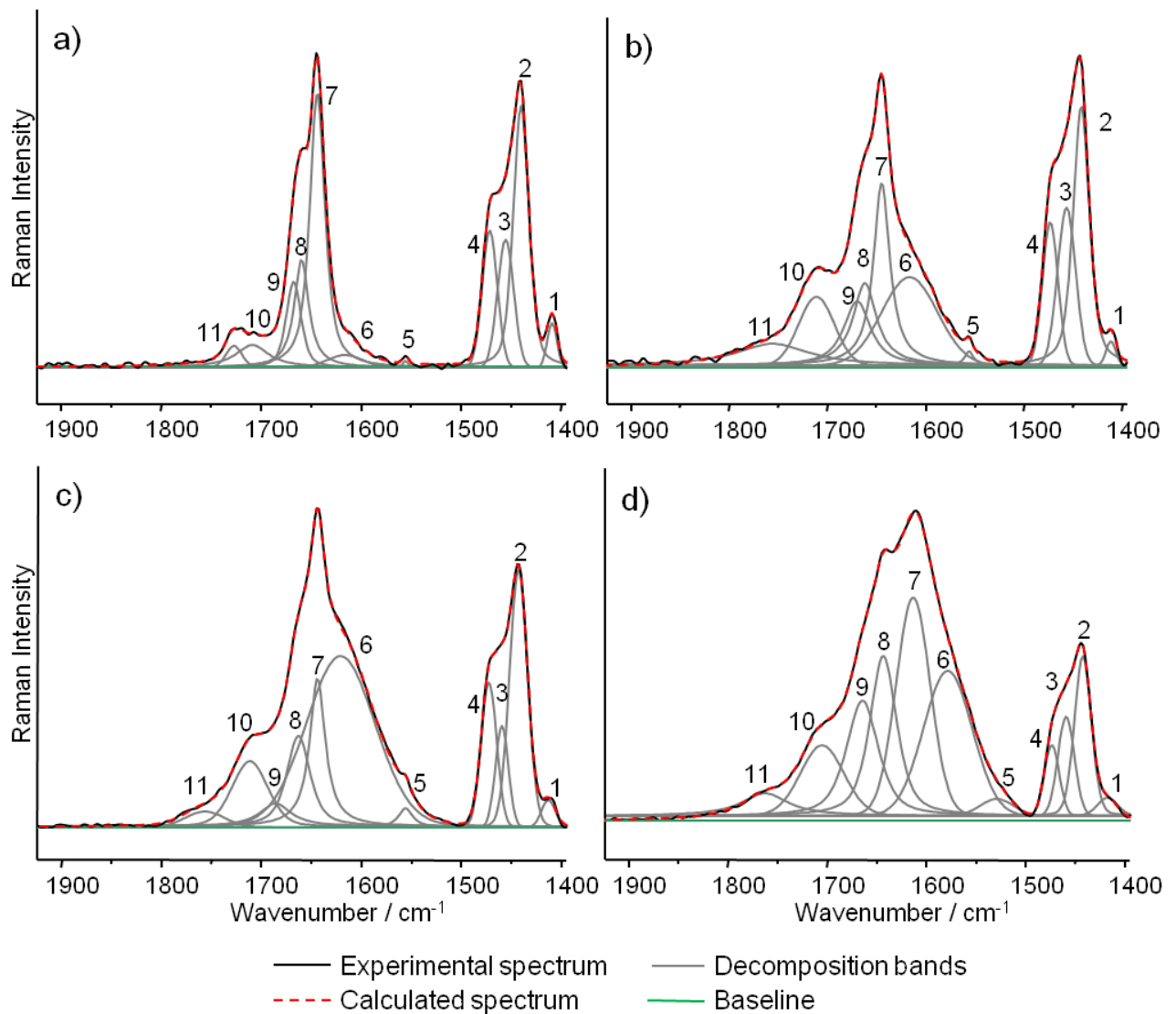
Fig. 5: Representative band decomposition of FT-Raman spectra for: a) yellow (MR1211) - internal sampling, b) yellow (MR1211) - external sampling, c) orange (MS5673) - external sampling and d) red (MR1234) - external sampling (same samples as Fig. 4). Decomposition bands are numbered from 1 to 11 according to their increasing positions.
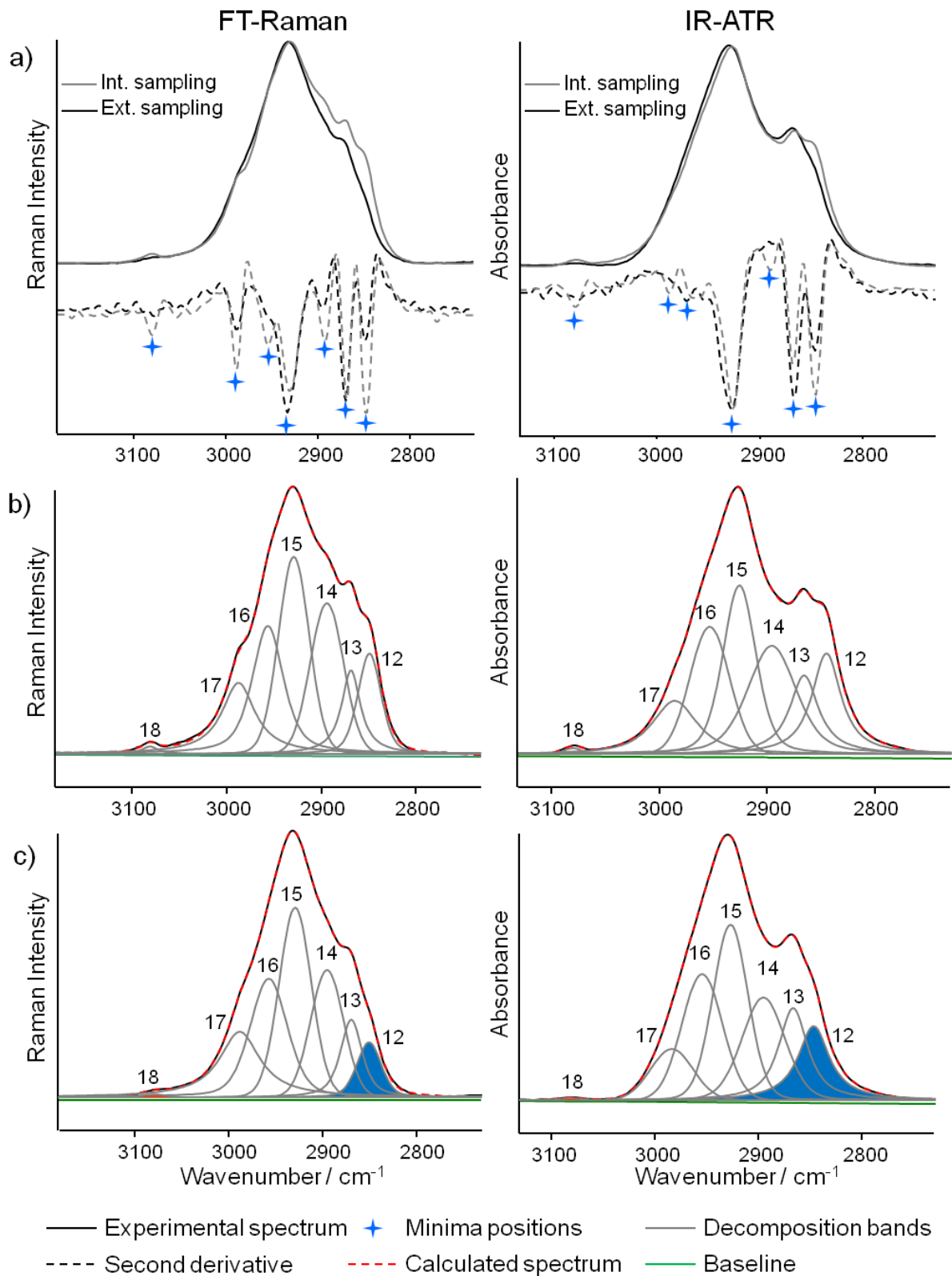
502

503

504
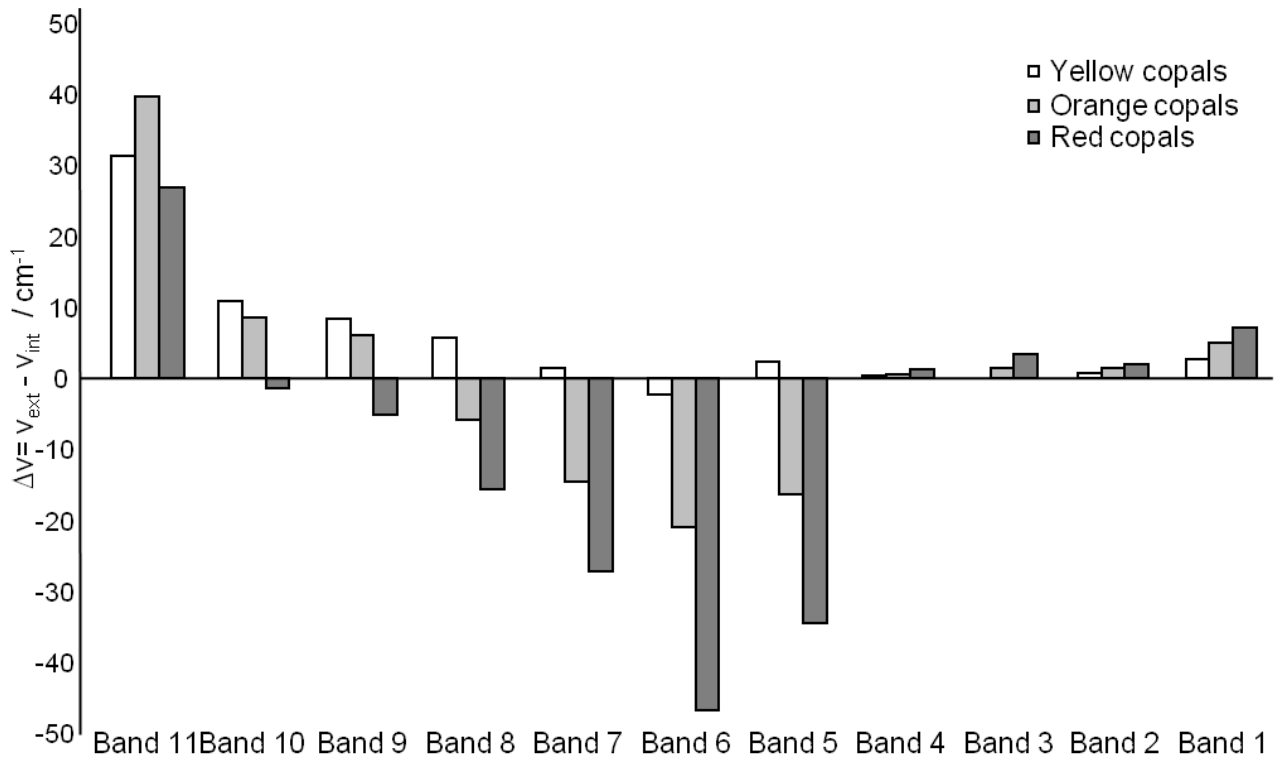
505

506

507 Fig. 6: Difference between the external and internal sample bands positions (Δv) of the 11

508 decompostion bands of the 1900-1400 cm^{-1} region. These are mean values for each group.
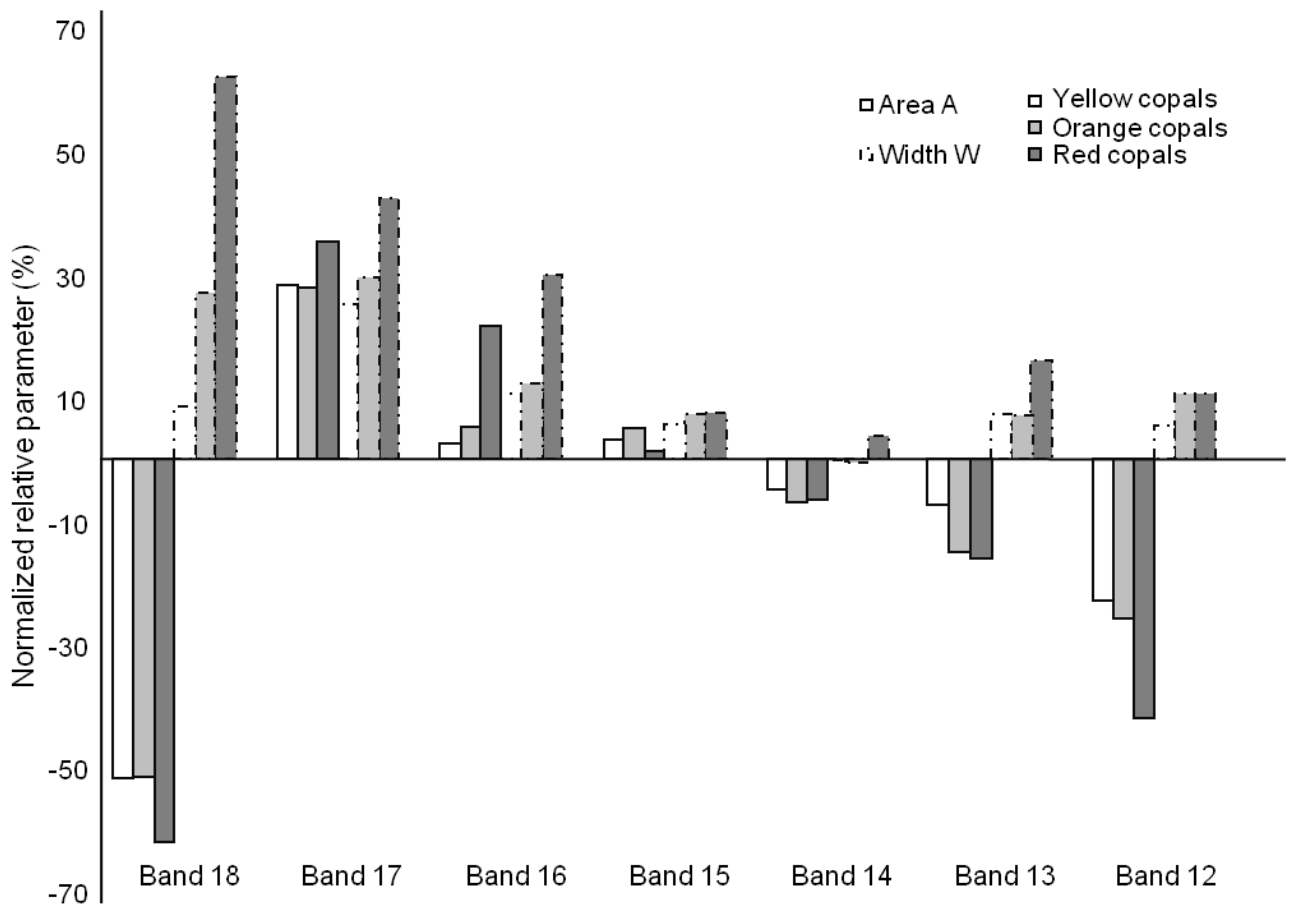
509

510

Fig. 7: ATR-IR and FT-Raman CH massifs for internal and external parts of a red sample (MR1214). a) Spectra and their second derivative, b) Decomposition of Raman and IR spectra of its internal part. c) Decomposition of Raman and IR spectra of its external part (colored bands are the most modified during ageing).
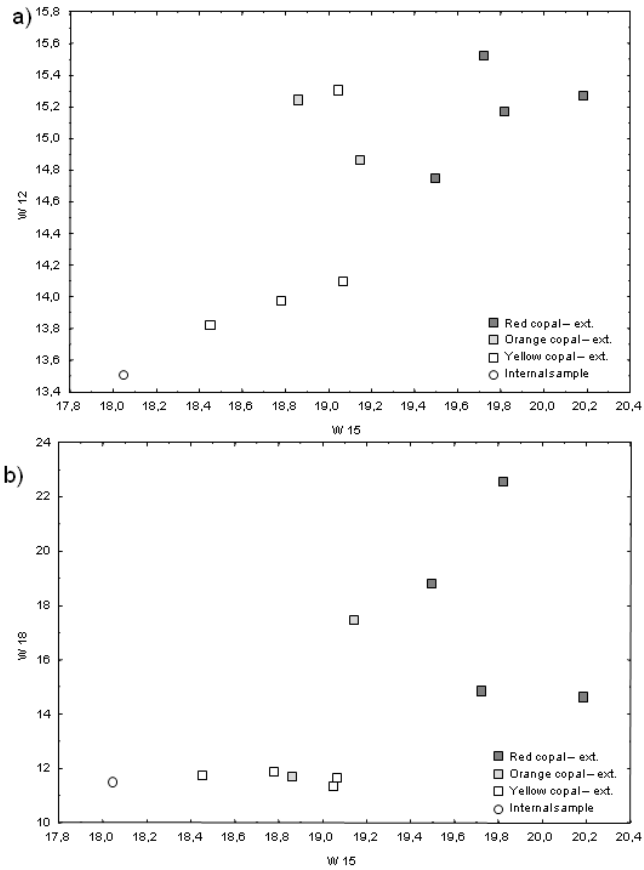
Fig. 8: Evolution of some bands parameters (the area A, and the width at half maximum W) between internal and external samplings, mean values for the 3 groups of copals. These normalized relative differences were calculated by the following equation (for each parameter i): $(i_{int.} - i_{ext.}) \times 100 / i_{int.}$

524
525
Fig. 9: Plots of parameters extracted from the CH massif band decomposition. A progression
in the colors can be observed on the diagonal of each graph which could define new alteration
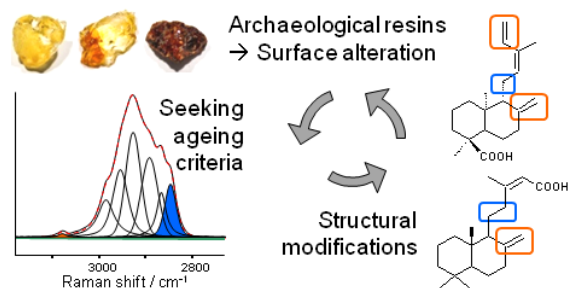indexes. a) Full width at half maximum of band 12 (W12) versus W15, and b) W18 versus
W15.
530

531 **Graphical TOC**

532

533

534

535

536 New insights about copal degradation mechanisms are introduced and relevant analytical

537 strategies for resinous substances through non destructive approaches by FT-Raman and

538 ATR-IR are presented.

539
540

541

542

543

544

545